Optimal Dynamic Discrimination of Similar Molecules through Quantum Learning Control†

Baiqing Li,‡ Gabriel Turinici,§ Viswanath Ramakrishna,|| and Herschel Rabitz*,‡

Department of Chemistry, Princeton University, Princeton, New Jersey 08544, INRIA Rocquencourt, 78153 Le Chesnay Cedex, France, and Department of Mathematical Sciences and Center for Signals, Systems and Communications, University of Texas at Dallas, P.O. Box 830688, Richardson, Texas 75083

Received: February 20, 2002; In Final Form: April 23, 2002

A paradigm for discriminating similar quantum systems in the laboratory is presented based on optimal control principles with the aid of closed loop learning algorithms. The optimal dynamic discrimination (ODD) process is simulated for a noninteracting mixture of up to three similar finite-dimensional quantum systems. The optimal control field giving rise to species discrimination, that considers the presence of field and observation noise, is deduced with a genetic algorithm (GA). The similar quantum systems yield distinct dynamics and detection signals, although influenced by the same control laser pulse. The ODD process is shown to operate by drawing on constructive and destructive interference effects to simultaneously maximize or minimize the signals from each of the species in the mixture. The ODD technique may have applications to the analysis and separation of possibly even complex chemical species.

I. Introduction

Similar molecules often may be characterized as sharing common chemical structures made up of the same atomic components. Such molecules are expected to have related Hamiltonians, and thus similar chemical and physical properties. Examples range from simple isotopic variants of diatomics (e.g., $^{79}Br_2$, $^{81}Br_2$) and isomers (e.g., *cis*- and *trans*-1,2-dichloroethylene) to highly complex molecules including those of biological relevance. A common need is to analyze or separate one molecular species in the presence of possibly many other similar agents. This problem often demands rapid, sensitive, and dependable identification or purification measures. Traditional approaches mainly focus on exploiting the subtle differences in the microscopic properties (e.g., enhancing spectroscopic resolution to differentiate close absorption peaks) or macroscopic properties (e.g., utilizing some form of chromatography for species separation) of the species.[1] These methods have seen wide applications, but they may all be characterized as "static" or "one-dimensional" with their capabilities being pushed to the limit. To enhance the ability to distinguish molecules, a new paradigm is proposed in this paper, aiming for optimal discrimination by actively amplifying the seemingly subtle differences between similar molecules.

The proposed optimal dynamic discrimination (ODD) approach exploits the richness of quantum molecular dynamics. Although the dynamics of similar quantum systems are governed by related Hamiltonians, each species could evolve in a distinct fashion under the same properly tailored external control. Thus the detection "dimension" is dynamically expanded, opening up the prospect for ODD. Exploiting ODD draws on emerging laser pulse shaping techniques combined with closed loop optimal learning control concepts.[2−10] Control theory was recently applied to separating an isotopic mixture of diatomic molecules,[11] and a closed loop learning control experiment was shown to be possible working with two separate molecular samples.[12] Closed loop learning control for ODD has attractive features, including the fact that little knowledge of the sample molecules is needed to determine tailored laser pulses capable of attaining selective dynamic evolution. Success in this regard requires only the existence of a clearly distinct one-to-one relationship connecting a specific laser pulse shape to the recorded signals from each species in the mixture. The ODD approach is not restricted by the complexity of the quantum systems to be discriminated, nor the intricacy of the quantum processes involved. The wave packets of the similar molecules in the system are excited by a common laser pulse, which is tailored with the goal of inducing signals (possibly detected with another common laser pulse) from only one species, while suppressing signals from all the others. Optimal control[13−15] techniques are potentially ideal tools for implementing ODD, as the underlying closed loop learning control process[6] inherently operates based on achieving discrimination between one dynamical process versus another. The special distinction here is seeking discrimination among *different* species. The manipulation of constructive and destructive interferences is at the heart of quantum control[8,10,13−17] This feature is present in the application of ODD to multiple species, but in this case constructive and destructive wave interferences can only occur *separately* within each species when attempting to attain overall control with a common laser field.

This paper aims to present some of the basic principles of ODD relevant to the experimental studies using learning control.[6,12] Simulations of the ODD process will be presented using simple few-level systems to illustrate the concepts. In section II, the ODD quantum control processes are described, and section III presents simulation results for two illustrations of up to three similar systems described by several discrete levels. Some brief conclusions are given in section IV.

† Part of the special issue "John C. Tully Festschrift".

* To whom correspondence should be addressed. E-mail: hrabitz@princeton.edu

‡ Princeton University.

§ INRIA Rocquencourt.

|| University of Texas at Dallas.

10.1021/jp0204657 CCC: $22.00
Published on Web 07/03/2002

II. Principles of Optimal Dynamic Discrimination

The analysis below aims to address the basic principles of ODD, and this will be done within a simple framework of seeking simultaneous control over multiple chemical/physical systems. Realistic systems will generally be more complex, but the basic principles should remain the same. The individual members of the set of similar systems subject to simultaneous ODD will be labeled by an identifying index $\nu = 1, 2, 3, ...$ Each species will be characterized by a finite number of active control states ($|\phi_0^\nu\rangle, |\phi_1^\nu\rangle, ..., |\phi_{N-1}^\nu\rangle$), which may interact with the control field $\epsilon_c(t)$, and an additional single detection state ($|\Gamma^\nu\rangle$), which is monitored to form a detection signal. This situation could, for example, correspond to the states $\{|\phi_i^\nu\rangle\}$ being in the ground electronic state and $|\Gamma^\nu\rangle$ being an excited vibronic state; many other variations may also arise in practical laboratory circumstances. For simplicity of presentation, these overall states are taken as orthonormal and form an $(N+1)$-dimensional Hilbert space; more complex settings where the number N of active control states ($|\phi_0^\nu\rangle, |\phi_1^\nu\rangle, ..., |\phi_{N-1}^\nu\rangle$) is not the same for all species can also be treated in a straightforward fashion. In a real environment the species would be at a finite temperature calling for dynamics described by the density matrix. To reveal the basic principles involved here, the dynamics of species ν will be described for simplicity by a wave packet $|\psi^\nu(t)\rangle$,

$$|\psi^\nu(t)\rangle = \sum_{i=0}^{N-1} c_i^\nu(t)|\phi_i^\nu\rangle + d^\nu(t)|\Gamma^\nu\rangle \quad \nu = 1, 2, 3, ... \quad (1)$$

where the coefficients $c_i^\nu(t)$ and $d^\nu(t)$ will evolve in time due to the influence of external fields. Generally, they are complex numbers subject to the following constraint:

$$\sum_{i=0}^{N-1} |c_i^\nu(t)|^2 + |d^\nu(t)|^2 = 1 \quad (2)$$

because of the normalization of $|\psi^\nu(t)\rangle$.

The total wave function $|\Psi(t)\rangle$ of all the species has the form $\prod_\nu |\psi^\nu(t)\rangle$ under the assumption that dynamical interaction between the systems relevant to the control processes may be neglected; in practice the closed loop learning control procedure would likely seek to optimally diminish the influence of any such interactions, and the presence of a surrounding solvent would aid this matter as well by tending to keep the species spatially separated.

Initially at time $-T$, the systems are all taken to be in their lowest energy level,

$$|\psi^\nu(-T)\rangle = |\phi_0^\nu\rangle \quad (3)$$

The collective sample is then exposed to a common laser pulse $\epsilon_c(t)$ over the interval $-T \le t < T$. This control laser pulse has frequency components that include only transitions among the first N levels $\{|\phi_i^\nu\rangle\}$ of each species such that at time T, the wave packets are described by

$$|\psi^\nu(T)\rangle = U_c^\nu(T, -T)|\psi^\nu(t)\rangle = \sum_{i=0}^{N-1} c_i^\nu(T)|\phi_i^\nu(t)\rangle \quad (4)$$

Here $U_c^\nu(T, -T)$ is the time propagator describing the control of system ν under the influence of the field $\epsilon_c(t)$. The term $\boldsymbol{c}^\nu(T) = \{c_i^\nu(T)\}$ is an N-dimensional complex vector with unit modulus because of the normalization of $|\pi^\nu(T)\rangle$,

$$||\boldsymbol{c}^\nu(T)|| = [\sum_{i=0}^{N-1} |c_i^\nu(T)|^2]^{1/2} = \{\sum_{i=0}^{N-1} [c_i^{\nu,\mathrm{Re}}(T)]^2 + [c_i^{\nu,\mathrm{Im}}(T)]^2\}^{1/2} = 1 \quad (5)$$

The superscripts Re and Im denote the real and imaginary part of $c_i^\nu(T)$, respectively. Equations 2 and 5 are consistent, as under the evolution driven by $\epsilon_c(t)$ the amplitude in the detection state $|\Gamma^\nu\rangle$ satisfies $d^\nu(T) = 0$, $-T \le t < T$.

The dynamics of each system is governed by its Schrödinger equation,

$$i\hbar\frac{\partial}{\partial t}|\psi^\nu(t)\rangle = [H_0^\nu - \mu^\nu\epsilon_c(t)]|\psi^\nu(t) \quad (6)$$

with

$$H_0^\nu|\phi_i^\nu\rangle = E_i^\nu|\phi_i^\nu\rangle$$
$$\langle\phi_i^\nu|\mu|\phi_j^\nu\rangle = \mu_{ij}^\nu\mu_{ij}^\nu = \mu_{ji}^\nu,\ \mu_{ii}^\nu = 0 \quad (7)$$

Here H_0^ν is the internal Hamiltonian and μ_{ij}^ν is an element of the dipole moment matrix which is assumed real for simplicity. After evolution under the control laser pulse $\epsilon_c(t)$, the systems are excited by a second detection laser pulse $\epsilon_d(t)$, whose frequency components couple the levels $|\phi_i^\nu\rangle$ to the detection state $|\Gamma^\nu\rangle$. The field $\epsilon_d(t)$ could be initiated at any time, including even before T; here it is assumed to act over the interval $T \le t \le T'$ with an associated time propagator $U_d^\nu(T + T', T)$. Thus the entire quantum propagation of species ν under the influence of the control and detection fields is

$$|\psi^\nu(T + T')\rangle = U_d^\nu(T + T', T)|\psi^\nu(T)\rangle = U_d^\nu(T + T', T)U_c^\nu(T, -T)|\psi^\nu(-T)\rangle \quad (8)$$

In the present work, the detection signal O^ν is simply taken as the final population in the detection state.

$$O^\nu[\epsilon_c(t),\epsilon_d(t)] = |\langle\Gamma^\nu|\psi^\nu(T + T')\rangle|^2 = |\sum_{i=0}^{N-1} c_i^\nu(T)\langle\Gamma^\nu|U_d^\nu(T + T', T)|\phi_i^\nu\rangle|^2 \quad (9)$$

The signal $O^\nu[\epsilon_c(t),\epsilon_d(t)]$ used for discrimination purposes could be either static and evaluated at a fixed T' or dynamic, as a time profile of $O[\epsilon_c(t),\epsilon_d(t), T']$ versus T'. A static signal is used in the present study, but dynamic signals have more flexibility and possibly offer higher degrees of discrimination. Both the control pulse $\epsilon_c(t)$ and the detection pulse $\epsilon_d(t)$ can be tailored for maximum ODD performance. To simplify the simulations here only the control pulse $\epsilon_c(t)$ is optimized to attain discrimination. For our purposes the pulse $\epsilon_d(t)$ need not be prescribed, as only the elements $\langle\Gamma^\nu|U_d^\nu|\phi_i^\nu\rangle$ enter into eq 9 and they are specified as real numbers D_i^ν (treating the numbers as complex does not alter the general structure of the discrimination formulation).

$$\langle\Gamma^\nu|U_d^\nu(T + T', T)|\phi_i^\nu\rangle = D_i^\nu \quad i = 0, 1, ..., N - 1 \quad (10)$$

$\boldsymbol{D}^\nu = \{D_i^\nu\}$ is an N-dimensional real vector and is expected to be similar for all the species due to their closely related nature.

Equation 9 now has the following simple form for the detection signal of system ν:

$$O^{\nu}[\epsilon_c(t)] = |\sum_{i=0}^{N-1} c_i^{\nu}(T)D_i^{\nu}|^2$$

$$= [\sum_{i=0}^{N-1} c_i^{\nu,\mathrm{Re}}(T)D_i^{\nu}]^2 + [\sum_{i=0}^{N-1} c_i^{\nu,\mathrm{Im}}(T)D_i^{\nu}]^2$$

$$= [\boldsymbol{c}^{\nu,\mathrm{Re}}(T)\cdot\boldsymbol{D}^{\nu}]^2 + [\boldsymbol{c}^{\nu,\mathrm{Im}}(T)\cdot\boldsymbol{D}^{\nu}]^2 \quad (11)$$

where the symbol $\cdot$ denotes a scalar product.

The signal $O^{\nu}[\epsilon_c(t)]$ from each of the similar systems $\nu = 1, 2, 3, ...$, is a functional of the same control field $\epsilon_c(t)$. Given the similarity of the species, application of an arbitrary field $\epsilon_c(t)$ might give similar dynamics and signal $O^{\nu}[\epsilon_c(t)]$ for all the species ν with little discrimination, and this outcome was observed to be the case in the simulations in section III. Rather, we seek to optimize $\epsilon_c(t)$ to achieve ODD. To attain ODD for species ξ over that of all other species $\nu \neq \xi$, one approach is to maximize signal $O^{\xi}[\epsilon_c(t)]$, while simultaneously minimizing the signals $O^{\nu}[\epsilon_c(t)]$ ($\nu \neq \xi$), through tailoring $\epsilon_c(t)$. A simple control functional for this purpose is

$$J[\epsilon_c(t)] = O^{\xi}[\epsilon_c(t)] - \sum_{\nu\neq\xi} O^{\nu}[\epsilon_c(t)] \quad (12)$$

where the goal is to maximize J. Other terms may be added to the functional to attain ancillary benefits (e.g., control field simplicity[18]).

Understanding the possible maximum and minimum values of the signals $O^{\nu}[\epsilon_c(t)]$ is important. Both the maximization and minimization of $O^{\nu}[\epsilon_c(t)]$ with respect to $\boldsymbol{c}^{\nu,\mathrm{Re}}(T)$ and $\boldsymbol{c}^{\nu,\mathrm{Im}}(T)$ are subject to the constraint in eq 5. This maximum signal is

$$O^{\nu,\max}[\epsilon_c(t)] = ||\boldsymbol{D}^{\nu}||^2 = \sum_{i=0}^{N-1}(D_i^{\nu})^2 \quad (13)$$

when

$$\boldsymbol{c}^{\nu,\mathrm{Re}}(T) = \alpha^{\nu}\boldsymbol{D}^{\nu},\ \boldsymbol{c}^{\nu,\mathrm{Im}}(T) = \beta^{\nu}\boldsymbol{D}^{\nu} \quad (14a)$$

$$(\alpha^{\nu})^2 + (\beta^{\nu})^2 = \frac{1}{||\boldsymbol{D}^{\nu}||^2} = \frac{1}{\sum_{i=0}^{N-1}(D_i^{\nu})^2} \quad (14b)$$

with α^{ν} and β^{ν} being constant functionals of the control field $\epsilon_c(t)$. The structure of eq 14a implies that the vectors $\boldsymbol{c}^{\nu,\mathrm{Re}}(T)$ and $\boldsymbol{c}^{\nu,\mathrm{Im}}(T)$ are either parallel or antiparallel to the vector $\boldsymbol{D}^{\nu}$, which is a demanding condition to arrange by $\epsilon_c(t)$. The minimal signal is

$$O^{\nu,\min}[\epsilon_c(t)] = 0 \quad (15)$$

which leads to

$$\boldsymbol{c}^{\nu,\mathrm{Re}}\cdot\boldsymbol{D}^{\nu} = 0,\ \boldsymbol{c}^{\nu,\mathrm{Im}}\cdot\boldsymbol{D}^{\nu} = 0 \quad (16)$$

implying that the vectors $\boldsymbol{c}^{\nu,\mathrm{Re}}(T)$ and $\boldsymbol{c}^{\nu,\mathrm{Im}}(T)$ are perpendicular to the vector $\boldsymbol{D}^{\nu}$. All pairs of vectors $\boldsymbol{c}^{\nu,\mathrm{Re}}(T)$ and $\boldsymbol{c}^{\nu,\mathrm{Im}}(T)$ in the $(N-1)$-dimensional space perpendicular to the vector $\boldsymbol{D}^{\nu}$ satisfy this condition. There is much more flexibility in satisfying eq 16 than the maximization conditions in eq 14. Thus the control objective in this realization of ODD is to steer species ξ to the state $|\psi^{\xi}(T)\rangle$ with $\boldsymbol{c}^{\xi}(T)$ satisfying eq 14, while steering all the other species $\nu \neq \xi$ to states $|\psi^{\nu}(T)\rangle$ with $\boldsymbol{c}^{\nu}(T)$ satisfying eq 16. Figure 1 graphically depicts the conditions in eqs 14 and 16 achieved under application of ODD through the influence of the optimal control field $\epsilon_c(t)$. Here a single vector $\boldsymbol{D}$ is shown, as all the vectors $\boldsymbol{D}^{\nu}$ could be nearly coincident for very similar systems. The demanding nature of eq 14 and the orthogonality freedom in eq 16 are evident from the geometry of the vectors. Achieving ODD for species ξ over all the other species $\nu \neq \xi$ thus calls for manipulating the vectors $\boldsymbol{c}^{\xi}$ and $\{\boldsymbol{c}^{\nu}\}$ ($\nu \neq \xi$) into these perpendicular orientations, respectively. The application of an arbitrary control field is likely to leave the set of vectors $\boldsymbol{c}^{\xi}$ and $\{\boldsymbol{c}^{\nu}\}$ ($\nu \neq \xi$) roughly aligned with resultant poor discrimination because of the similarities of the species. Thus the control field has to be determined carefully.

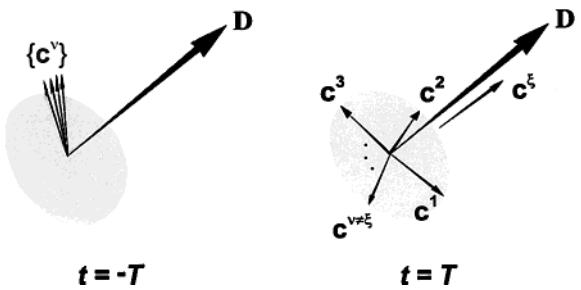

Figure 1. Graphic depiction of the quantum optimal dynamic discrimination mechanism contained in eqs 14 and 16. The signal for species ξ is to be maximized while those of $\nu \neq \xi$ are to be minimized. The control process can be understood as the manipulation of the wave function component vectors $\boldsymbol{c}^{\nu}(t)$. Initially at $t = -T$, the vectors $\{\boldsymbol{c}^{\nu}(-T)\}$ for all species ν are nearly parallel to each other. At the end of the optimal control process ($t = T$), the vector $\boldsymbol{c}^{\xi}(T)$ is parallel to the vector $\boldsymbol{D}$, while the background species have vectors $\{\boldsymbol{c}^{\nu}(T)\}$ ($\nu \neq \xi$) perpendicular to $\boldsymbol{D}$. Here a single vector $\boldsymbol{D}$ is used for illustration, as $\boldsymbol{D}^{\nu} \approx \boldsymbol{D}$ for all similar chemical species ν. A vector $\boldsymbol{c}$ is understood to have for both real $\boldsymbol{c}^{\mathrm{Re}}$ and imaginary $\boldsymbol{c}^{\mathrm{Im}}$ parts.

A basic question is whether the multiple optimization goals above can be achieved simultaneously. In other words, are these similar systems simultaneously controllable with a single laser pulse? Controllability in the present context is defined as the existence of at least one control field $\epsilon_c(t)$ capable of steering a quantum system from a certain initial state to a certain final state within finite time. The system here is understood to be described by the full Hamiltonian consisting of the ensemble $\{H_0^{\nu} - \mu^{\nu}\epsilon_c(t)\}$ for all species, with controllability being simultaneously sought for all of the states $|\psi^{\nu}(t)\rangle$. An analysis of the mathematics involved will be considered in a following work.[19] However, all of the cases investigated in section III were fully controllable, so that the extrema in eqs 14 and 16 can in principle be achieved by at least some control field within finite time. This point of certainty can be used to assess the effectiveness of the learning algorithm in the ODD simulations in section III. Nevertheless, no precise value for the duration of the control pulse, T, allowing simultaneous control of all the species is available via theoretical controllability analysis; moreover, it is generally expected that the time for simultaneously controlling multiple systems may be longer than that required for controlling only one system.

III. Simulations of Optimal Dynamic Discrimination

The simulations below aim to explore some of the basic concepts of ODD and its capabilities. Realistic laboratory cases[2−5,7,9,12] will likely be far more complex, but simple systems have often proved useful[6,13−15] in capturing the essence of quantum control techniques. Two cases are simulated here: (1)

two similar systems with four levels in their active control space, and (2) three similar systems with ten levels in their active control space. In the examples no specific regular relations were imposed between the energy levels and the transition dipoles, following what would likely be the situation in realistic cases where optimal discrimination would be most useful. Thus, the indicated quantum numbers should just be viewed as state labels in the present work. The numerical values below have the units of fs for time, rad/fs for frequency and energy, V/Å for electric field, and 10^{-20} CÅ for electric dipole moment.

In all the simulations the control field is constrained to the following form:

$$\epsilon_c(t) = \epsilon_0 \exp[-(t/\sigma)^2]\sum_{l=1}^{L} a_l \cos(\omega_l t + \theta_l) \qquad (17)$$

in which ϵ_0, σ, and all the frequencies ω_l are fixed beforehand, while all the amplitudes a_l and phases θ_l are control variables to be optimized over the intervals [0,1] and [0,2π], respectively. Because of the restrictions on duration, amplitude, and shape of the excitation pulse, reaching the maximal possible ODD signals is not guaranteed. The power spectrum of each frequency component of $\epsilon_c(t)$ in eq 17 is a finite-width Gaussian-shaped peak $\exp[-(\omega-\omega_l/(2/\sigma)^2]$ centered at ω_l, with a half width of $1.67/\sigma$. The functional $J[\epsilon_c(t)]$ is now reduced to a function of the control variables $\mathbf{a} = \{a_l\}$ and $\boldsymbol{\theta} = \{\theta_l\}$.

$$J[\epsilon_c(t)] = J(\mathbf{a},\theta) \qquad (18)$$

The simulations for finding the ODD fields were done with a genetic algorithm (GA)[20] along the lines of current experimental practice in a variety of quantum control applications,[2−9,12] although other learning algorithms could be used. In addition, some cases also included control field noise to explore its impact on ODD performance. The adopted GA software package, GALib[21] was modified for our specific purposes. In the following simulations, a steady-state GA is implemented and real-valued genomes, instead of binary genomes, are used to represent the parameters to be optimized. The operating parameters for the GA are as follows: the population size is 100, the number of generations is less than 2000, the mutation probability is 5%, the crossover probability is 90%, and the generation-to-generation replacement percentage is 90%.

1. Two Similar Four-Level Systems. This simulation involves two similar systems, A and B, and both have four active control levels. The energies E_i, the transition dipole moments μ_{ij}, and the parameters characterizing the detection process D_i of A are fixed and specified in ref 22, while those of B are randomly chosen to be close to those of A. The goal is to induce a maximum signal from A while simultaneously quenching the signal from B, as described in section II and specified through maximization of J^{A-B}.

$$J^{A-B}(\mathbf{a},\boldsymbol{\theta}) = O^A(\mathbf{a},\boldsymbol{\theta}) - O^B(\mathbf{a},\boldsymbol{\theta}) \qquad (19)$$

The control pulse in eq 17 has the parameters $T = 100$, $\sigma = 40$, and $\epsilon_0 = 1$. The frequencies ω_l correspond to all possible transitions between the active control states of A and B respectively, so that $L = 12$ in eq 17 covers the transitions of both species. The possible maximum of J^{A-B} is 0.2125 calculated with the parameters D_i^A [22] using eq 13.

In the first test, B is chosen to be similar to A[22] with the randomly set parameters in ref 23. The maximum value of J^{A-B} reached in the simulation is 0.2124 ($O^A = 0.2124$, $O^B = 1.0 \times 10^{-5}$, corresponding to 99.95% discrimination[24]). Figure 2 shows

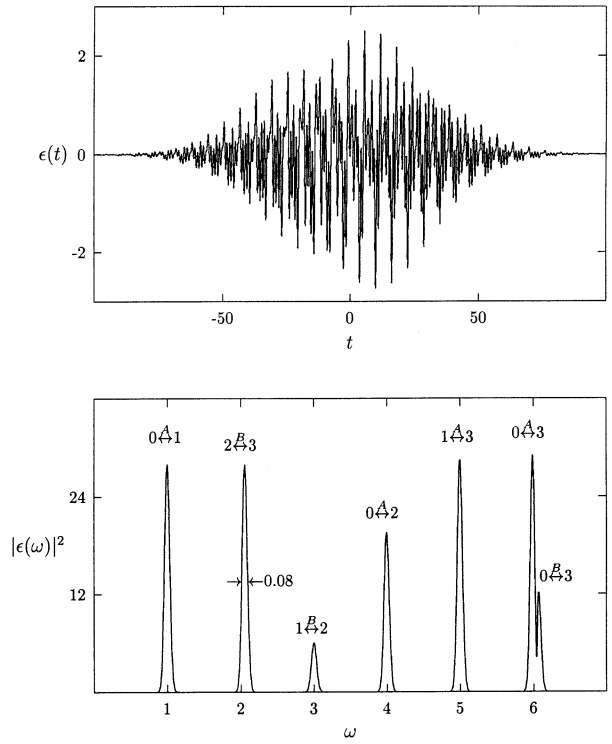

Figure 2. Time profile and power spectrum of the optimal pulse that maximizes J^{A-B} in the first test of the systems with four active control states in section III.1. The power spectrum is in arbitrary units. The lines as labeled correspond to specific identified transitions in A or B, but the corresponding transitions for the partner species also lie under the indicated power spectral bandwidths. This point is evident from the corresponding transition frequencies for A ($\omega_{01}^A = 1$, $\omega_{23}^A = 2$, $\omega_{12}^A = 3$, $\omega_{02}^A = 4$, $\omega_{13}^A = 5$, and $\omega_{03}^A = 6$) and for B ($\omega_{01}^B = 1.0033$, $\omega_{23}^B = 2.0587$, $\omega_{12}^B = 3.0027$, $\omega_{02}^B = 4.006$, $\omega_{13}^B = 5.0614$, and $\omega_{03}^B = 6.0647$). Discrimination of A and B is achieved by exploiting constructive and destructive dynamic interferences manifested through the subtle differences between the two molecules.

the optimal control pulse $\epsilon_c(t)$ and its power spectrum. By assigning the peaks in the spectrum to the transitions of either A or B, the paths taken by A (i.e., transitions 0↔1, 0↔2, 1↔3, and 0↔3) and B (i.e., transitions 2↔3, 1↔2, and 0↔3) appear to be quite disparate. However the actual ODD mechanism is more subtle, as almost all the pairs of transition frequencies for A and B (calculated using the energy differences from the data in refs 22−23, see the caption of Figure 2) are well within the half widths of 0.04 rad/fs evident in Figure 2. In addition, dynamic Stark shifting (i.e., power broadening) of the levels by the field will further enhance the subtle relationship between the impact of the control on the dual dynamics of A and B. Thus, each frequency component in Figure 2 labeled by a transition of a particular species A or B will actually have some direct influence on the same transition in the other corresponding species. This circumstance illustrates the common situation where simple spectral filtering alone cannot satisfactorily discriminate one complex species from another.

Successful quantum control is best achieved through the manipulation of destructive and constructive interferences to favor one outcome over that of other possibilities.[8,10] Table 1 shows that this is the underlying reason for the successful performance of ODD in this example. It is evident that the amplitude for the states of A and B are manipulated in a subtle fashion such that upon projection to the detection states $|\Gamma^A\rangle$ and $|\Gamma^B\rangle$ the contributions from all the active control states to the signal O^A constructively add up, but destructively cancel

TABLE 1: Mechanism of Quantum Optimal Dynamic Discrimination

	species A		species B	
j	c_j^{A} [a]	$c_j^{A}D_j^{A}$ [b]	c_j^{B} [a]	$c_j^{B}D_j^{B}$ [b]
0	−0.065+0.083i	0.003−0.004i	0.001−0.423i	0.021i
1	0.498−0.712i	0.199−0.285i	0.228+0.023i	0.091+0.009i
2	0.246−0.354i	0.049−0.071i	−0.608−0.376i	−0.121−0.075i
3	−0.134+0.171i	0.014−0.017i	−0.283−0.420i	0.028+0.042i
$\sum_{j=0}^{N-1} c_j D_j$ [c]	not applicable	0.265−0.377i	not applicable	−0.002−0.003i

[a] Wave packet components of active control states. [b] Components projected upon the detection state. [c] The observed signal of A is maximized and that of B is minimized by constructive and destructive interferences in the respective detection states. This case is the first example in section III.1. The mechanism for discriminations in the other examples similarly draws on interference effects.

out for O^{B}, which explains the maximal signal for A and the minimal signal for B. This result demonstrates that the conditions for maximal and minimal signals given in eqs 14 and 16 and illustrated in Figure 1 are equivalent to exploiting constructive and destructive interferences, respectively. Furthermore, this case also shows that A and B would not be properly discriminated by conventional spectroscopic means if the population in the detection states $|\Gamma^{A}\rangle$ and $|\Gamma^{B}\rangle$ were monitored, as without suitable control the differences between the signals O^{A} and O^{B} are not enough for optimal discrimination. In the present example sufficiently high-resolution spectroscopy from the ground state would permit discrimination. However, the purpose of the present illustrations is to introduce a capability for dynamic discrimination where spectral approaches are not adequate. Thus the finite bandwidth of the present control $\epsilon_c(t)$ introduces complexities of the type expected in treating realistic molecular situations.[2−5,7,9,11,12]

Since the transition frequencies of A and B are close and the power spectrum of the excitation pulse is a collection of Gaussian peaks centered around them, there inevitably are overlaps between the corresponding transitions of A and B, as discussed above and shown in Figure 2. For cases where A and B are so different that there is no overlap at all, and the dynamic Stark effect does not induce significant overlap between the corresponding transitions, then the species A and B may be independently controlled based on frequency alone. In this circumstance, an overall control $\epsilon_c(t) = \epsilon_c^{A}(t) + \epsilon_c^{B}(t)$ made up of a portion $\epsilon_c^{A}(t)$ that maximizes the signal O^{A} and a portion $\epsilon_c^{B}(t)$ that minimizes the signal O^{B} will produce an optimal value for J^{A-B}. At the other extreme, if A and B are the same system, then their transitions fully overlap, and clearly no discrimination is possible. Between these two extremes, when there are (a) spectral overlaps, (b) similar transition dipoles, and (c) nearly the same transfer couplings $\boldsymbol{D}^{\nu}$ to the observation state, as in the above test case, the situation is quite complex requiring that the ODD control pulse $\epsilon_c(t)$ be determined working *simultaneously* with A and B, instead of being synthesized from the two separate optimal pulses that individually maximize O^{A} and minimize O^{B}. Under closed loop optimal control, even dynamic power broadening effects might be turned into a beneficial process to aid the discrimination. Cases of increasingly similar spectra are naturally expected to make it more difficult to achieve good quality discrimination. To test this issue, two other B systems, described in refs 25 and 26, were considered, whose energy levels are more similar to A than the system B[23] in the first test; the system B[26] is more similar to A than that of B.[25] Additionally, it was found in these examples that the differences between the dipole moments and D_i values of A and B did not have a significant effect on the optimization, so the dipole moments and D_i values for B[25,26] are the same as those of B.[23] The maximal value of J^{A-B} found for B[25,26] is in accordance with the degree of similarity between A and B. The maximal value of J^{A-B} found for B[25] is 0.2099 (98.77% discrimination) and for B[26] is 0.1686 (79.34% discrimination). These results are not the maximum achievable values with arbitrary control pulses (i.e., the combined systems in all the cases are fully controllable[19]), primarily due to the restrictions on the duration, shape, and amplitude of the control pulses as well possibly because the GA did not fully explore the available control space.

One complexity involved in laboratory control experiments is the presence of laser pulse noise and observation errors, both of which can have several sources. If the optimal pulse is not robust to such noise, then the ODD process will be of less value. In practice, signal averaging would be performed in the laboratory to report[18]

$$\tilde{J}^{A-B} = \langle J^{A-B} \rangle_M \tag{20}$$

which is the average of M repeated runs with nominally the same control field. As a simulation of this process in the case of A[22] and B[23] for each field called for by the GA, the amplitudes and phases were randomly chosen around those of the candidate pulse. For the amplitudes, the fluctuations had a relative standard deviation of 1%. For the phases, the fluctuations had an absolute standard deviation of 0.05 rad. The combined observed signal J^{A-B} also had an absolute standard deviation of 0.002 (i.e., corresponding to an observation error of approximately 1%). M is chosen as 100, and the maximal value of $\tilde{J}^{A-B}$ reached was 0.2067 (97.3% discrimination). Of the 100 random pulses tested around the final optimal pulse, 54 of them yielded higher J^{A-B} than $\tilde{J}^{A-B}$ ($\sigma^{+} = 3.5 \times 10^{-4}$) and 46 yielded lower J^{A-B} than $\tilde{J}^{A-B}$ ($\sigma^{-} = 4.6 \times 10^{-4}$). The quality of the discrimination is still excellent, and the standard deviation of $\tilde{J}^{A-B}$ is smaller than that of the control and observation errors, indicating that control pulses can be found that are both optimal for discrimination and robust. As argued before[18] and demonstrated here, the use of signal averaging while seeking optimality produces an inherent degree of robustness to field noise. However, if large amplitude noise fluctuations remain a problem, then minimization of the standard deviation of J^{A-B} with respect to field noise can be explicitly added to the cost to further enhance robustness.[18]

In addition to control field noise and observation errors, the molecules may be subjected to various environmental effects including intermolecular interactions for samples at sufficient densities, and various other line broadening processes. These processes can compromise the constructive/destructive interference beneficial to the performance of ODD. Nevertheless, this situation does not necessarily suggest a breakdown of ODD, as alternative discrimination mechanisms can arise including the beneficial manipulation of decoherence among the family of similar quantum systems. Simulations of ODD in this regime call for a suitable density matrix formulation, and laboratory studies already operate in this domain.[12]

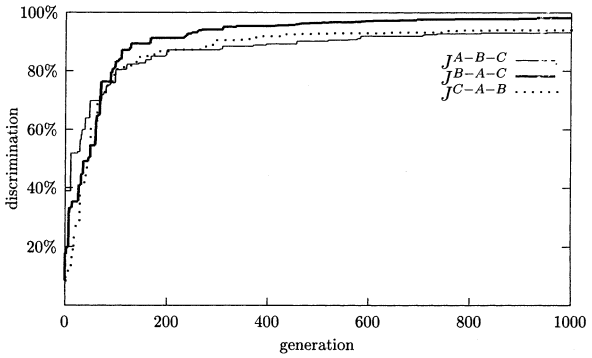

Figure 3. Evolution of the achieved maximum discrimination versus the generation of the GA for the three cases A−B−C, B−A−C, and C−A−B in section III.2, where the signal of the first species is to be maximized over that of the others. Initially the discrimination is only moderate, and the maximum discrimination in each generation increases monotonically, because with a steady-state GA, the best control field from the previous generation is always retained.

2. Three Similar Ten-Level Systems. This illustration involves three similar systems, A, B, and C, each of which has 10 states in its active control spaces. The energy levels, E_i, dipole moments, μ_{ij}, and D_i values for A are listed in ref 27, and those of B and C are arranged (not shown here) within close proximity to those of A as in the examples of section III.1 As mentioned earlier, the characteristics of A[27] were chosen rather arbitrarily. The following three functions are separately maximized:

$$J^{A-B-C}(\mathbf{a},\boldsymbol{\theta}) = O^{A}(\mathbf{a},\boldsymbol{\theta}) - O^{B}(\mathbf{a},\boldsymbol{\theta}) - O^{C}(\mathbf{a},\boldsymbol{\theta})$$

$$J^{B-A-C}(\mathbf{a},\boldsymbol{\theta}) = O^{B}(\mathbf{a},\boldsymbol{\theta}) - O^{A}(\mathbf{a},\boldsymbol{\theta}) - O^{C}(\mathbf{a},\boldsymbol{\theta})$$

$$J^{C-A-B}(\mathbf{a},\boldsymbol{\theta}) = O^{C}(\mathbf{a},\boldsymbol{\theta}) - O^{A}(\mathbf{a},\boldsymbol{\theta}) - O^{B}(\mathbf{a},\boldsymbol{\theta}) \quad (21)$$

Each case attempts to induce a maximal signal exclusively from the first of the three species while suppressing signals from the other two (e.g., maximize O^{A} for J^{A-B-C} while minimizing O^{B} and O^{C}). The control pulse $\epsilon_c(t)$ in each case had the characteristic variables $T = 500$, $\sigma = 200$, and $\epsilon_0 = 1$. From the experience learned through the simulations described in section III.1, the closer the corresponding transitions of A, B, and C, the more difficult it will be to achieve the desired discrimination. All the possible transitions between pairs of levels were carefully screened, and only the 16 most distinct transitions in each species were retained for control purposes. This leaves a total of $L = 48$ terms in eq 17 corresponding to 96 control variables; in principle, the GA would have acted as well to discover this reduced set of significant variables and the preselection was done just to accelerate the search process. The allowed transitions permit all of the levels to be connected either directly or indirectly, so that arbitrary amplitude transfer within each species is still possible in principle. J^{A-B-C}achieved a maximal value of 0.7861 ($O^{A} = 0.7908$, $O^{B} = 0.0026$, $O^{C} = 0.0021$) corresponding to 93.8% discrimination. J^{B-A-C} was maximized to the value of 0.8263 (98.2% discrimination), and J^{C-A-B} to 0.7969 (94.2% discrimination). The evolution of the achieved maximum discrimination throughout the GA optimization process is displayed in Figure 3 as a function of generation. Each species was separately detected to a high degree of quality in the presence of the other two competing species. A detailed examination of the wave function amplitudes at $t = T$ shows that ODD is again achieved through subtle use of constructive and destructive interferences. Similar to the situation in section III.1, the fields in these three cases have significant contributions at frequencies producing simultaneous overlaps with all the species transitions. Full 100% discrimination is not achieved mainly because of the restrictions on the control pulse, which will always be present in some form in the laboratory. As a final more difficult case, we set the levels 3, 4, 5, and 6 of A, B, and C to have exactly the same corresponding energies, as well as the same dipole moment matrix elements between them and the same corresponding D_i values. Nevertheless, better than 85% discrimination was achieved.

3. Comments on Optimal Dynamic Discrimination. Although the test cases are much simpler in section III.1 and section III.2 than many real systems of interest in the laboratory, they suffice for illustrating the ODD concept. Importantly, application of ODD does not require any detailed information about the individual systems, and systems of high complexity (i.e., characterized by broad overlapping spectra) should be amenable to treatment. Only experimental studies will be able to discern the practical degrees of discrimination possible in any particular case. This effort should be facilitated by the fact that essentially the same laboratory setups being used for closed loop learning control of chemical reactivity and other applications[2,4−7,9] may be redirected for ODD. A recent closed loop experimental study discriminating two dye molecules in a mixture is indicative that this can be done.[12]

The high repetition rate and stability of laser sources and modulators, along with fast signal detection should permit the exploration of thousands or more trial discrimination pulses over a reasonable laboratory time frame of even minutes. Efficient learning algorithms are still necessary, since the optimization problem is nominally of exponential complexity in the number of control variables due to the highly complex landscape of the control functional. In all of the simulations in this work, the random pulses used to initialize the GA give very low to moderate discrimination, reflecting the basic similarity of the molecules. With the progress through the GA generations, ever more discrimination was realized until very high quality was achieved as shown in Figure 3. This behavior also speaks to the need to include the signals $O^{\nu'}$ along with O^{ν} in eq 12; for typical circumstances only optimizing on O^{ν} will inevitably produce undesirable contamination from $O^{\nu'}$ ($\nu' \neq \nu$) signals. The optimal management of the entire sample simultaneously is the essence of the ODD process. Although the number of control variables went from 24 to 96 in the A−B and A−B−C cases, the learning algorithm showed no significant slowdown in finding the optimal results. A further issue to explore is the influence of the amount of each species present in the sample upon the performance of ODD.

IV. Conclusion

Optimal control of quantum systems using closed-loop learning algorithms directly in the laboratory is a general procedure with demonstrated successful control over a variety of chemical and physical phenomena.[2−5,7,9,12] The simulations in this paper suggest that quantum ODD might be a practical tool in many cases. The simulations used one particular type of signal, and in principle any signal sensitive to the evolving quantum states could be employed. This flexibility is one significant feature of the ODD procedure.

A key characteristic of ODD is its ability to draw on the richness of quantum dynamics behavior to magnify the differences between seemingly similar systems. Utilizing quantum interference phenomena plays a crucial role in ODD. Accordingly, quantum ODD has the potential of achieving higher sensitivity, compared with the traditional "static" discrimination approaches.

We hope that this paper stimulates a thorough laboratory testing of the ODD capabilities. Possible applications include detection/separation of isotopes[11] and isotope labeled molecules, discrimination of molecules with similar spectroscopic features,[12] etc. Many practical issues regarding laser source characteristics, signal detection, and the nature of the samples need to be investigated, but their laboratory explorations are feasible. A variety of optical and mass spectroscopic detection[7] approaches should be applicable to implement ODD.

Acknowledgment. B. Li and H. Rabitz thank the ARO, NSF, and the Program in Plasma Science and Technology at Princeton University for support of this research. V. Ramakrishna acknowledges NSF support from grant DMS 0072415. B. Li also thanks Drs. T.-S. Ho and W. Zhu for reading the manuscript, and Dr. J. M. Geremia, X.-J. Feng, and A. Mitra for valuable discussions. We especially acknowledge the preliminary work of Dr. H. Zhang using local optimal control theory for studies of isotope separation.[28]

References and Notes

(1) *Encyclopedia of Separation Science*; Wilson, I. D., Adlard, E. R., Cooke, M., Poole, C. F., Eds.; Academic Press: San Diego, CA, 2000.

(2) Assion, A.; Baumert, T.; Bergt, M.; Brixner, T.; Kiefer, B.; Seyfried, V.; Strehle, M.; Gerber, G. *Science* **1998**, *282*, 919.

(3) Bardeen, C. J.; Yakovlev, V. V.; Wilson, K. R.; Carpenter, S. D.; Weber, P. M.; Warren, W. S. *Chem. Phys. Lett.* **1997**, *280*, 151.

(4) Bartels, R.; Backus, S.; Zeek, E.; Misoguti, L.; Vdovin, G.; Christov, I. P.; Murnane, M. M.; Kapteyn, H. C. *Nature* **2000**, *406*, 164.

(5) Hornung, T.; Meier, R.; Zeidler, D.; Kompa, K. L.; Proch, D.; Motzkus, M. *Appl. Phys. B* **2000**, *71*, 277.

(6) Judson, R. S.; Rabitz, H. *Phys. Rev. Lett.* **1992**, *68*, 1500.

(7) Levis, R. J.; Menkir, G.; Rabitz, H. *Science* **2001**, *292*, 709, and references therein.

(8) Rabitz, H.; de Vivie-Riedle, R.; Motzkus, M.; Kompa, K. *Science* **2000**, *288*, 824, and references therein.

(9) Vajda, Š.; Bartelt, A.; Kapostaa, E. C.; Leisnerb, T.; Lupulescua, C.; Minemotoc, S.; Rosendo-Franciscoa, P.; Wöste, L. *Chem. Phys.* **2001**, *267*, 231.

(10) Warren, W. S.; Rabitz, H.; Dahleh, M. *Science* **1993**, *259*, 1581, and references therein.

(11) Leibscher, M.; Averbukh, I. S. *Phys. Rev. A* **2001**, *6304*, 3407.

(12) Brixner, T.; Damrauer, N. H.; Niklaus, P.; Gerber, G. *Nature* **2001**, *414*, 57.

(13) Kosloff, R.; Rice, S. A.; Gaspard, P.; Tersigni, S.; Tannor, D. J. *Chem. Phys.* **1989**, *139*, 201.

(14) Peirce, A.; Dahleh, M.; Rabitz, H. *Phys. Rev. A* **1988**, *37*, 4950.

(15) Shi, S.; Woody, A.; Rabitz, H. *J. Chem. Phys.* **1988**, *88*, 6870.

(16) Brumer, P.; Shapiro, M. *Philos. Trans., R. Soc. London A* **1997**, *355*, 2409.

(17) Gordon, R. J.; Rice, S. A. *Annu. Rev. Phys. Chem.* **1997**, *48*, 601.

(18) Geremia, J. M.; Zhu, W.; Rabitz, H. *J. Chem. Phys.* **2000**, *113*, 3960.

(19) Turinici, G.; Ramakrishna, V.; Li, B.; Rabitz, H., submitted to *Phys. Rev. A.*

(20) Goldberg, D. E. *Genetic Algorithms in Search, Optimization, and Machine Learning*; Addison-Wesley: Reading, MA 1989.

(21) The source code of the genetic algorithm software package, GALib, used in the simulations is available at http://lancet.mit.edu/ga/.

(22) The variables characterizing A in the two species example in section III.1: $E_0^A = 0.0$; $E_1^A = 1.0$; $E_2^A = 4.0$; $E_3^A = 6.0$; $\mu_{01}^A = 1.6$; $\mu_{02}^A = 0.3$; $\mu_{03}^A = 0.7$; $\mu_{12}^A = 0.8$; $\mu_{13}^A = 0.2$; $\mu_{23}^A = 0.9$; $D_0^A = -0.05$; $D_1^A = 0.4$; $D_2^A = 0.2$; $D_3^A = -0.1$.

(23) The variables characterizing B in the two species example in section III.1: $E_0^B = -0.0325$; $E_1^B = 0.9708$; $E_2^B = 3.9735$; $E_3^B = 6.0322$; $\mu_{01}^B = 1.5896$; $\mu_{02}^B = 0.2977$; $\mu_{03}^B = 0.6996$; $\mu_{12}^B = 0.8011$; $\mu_{13}^B = 0.1985$; $\mu_{23}^B = 0.894$; $D_0^B = -0.0503$; $D_1^B = 0.3966$; $D_2^B = 0.1987$; $D_3^B = -0.1002$.

(24) The percentage discrimination is defined as the actually achieved maximum of J divided by the possibly achievable maximum of J, which can be calculated using eqs 13 and 15.

(25) A more demanding case for B in the two species example in section III.1: $E_0^B = 0.0159$; $E_1^B = 1.0173$; $E_2^B = 4.0108$; $E_3^B = 5.9865$. The other variables are the same as in ref 23.

(26) The most demanding case for B in the two species example in section III.1: $E_0^B = 0.0052$; $E_1^B = 1.007$; $E_2^B = 3.9943$; $E_3^B = 5.99$. The other variables are the same as in ref 23.

(27) The variables characterizing A in the three species example in section III.2: $E_0^A = 2.9923$; $E_1^A = 5.9973$; $E_2^A = 8.6744$; $E_3^A = 10.9953$; $E_4^A = 13.0022$; $E_5^A = 14.6376$; $E_6^A = 15.9601$; $E_7^A = 16.9411$; $E_8^A = 17.5713$; $E_9^A = 17.8630$; $\mu_{01}^A = 9.76 \times 10^{-2}$; $\mu_{02}^A = -3.66 \times 10^{-2}$; $\mu_{03}^A = 4.9041 \times 10^{-1}$; $\mu_{04}^A = 6.4 \times 10^{-3}$; $\mu_{05}^A = -6.5 \times 10^{-2}$; $\mu_{06}^A = 6.077 \times 10^{-1}$; $\mu_{07}^A = -1.4 \times 10^{-3}$; $\mu_{08}^A = 1.3278 \times 10^{-2}$; $\mu_{09}^A = -9.29 \times 10^{-2}$; $\mu_{12}^A = 7.036 \times 10^{-1}$; $\mu_{13}^A = 4 \times 10^{-4}$; $\mu_{14}^A = -3.4673 \times 10^{-3}$; $\mu_{15}^A = 2.1741 \times 10^{-2}$; $\mu_{16}^A = -1.2250 \times 10^{-1}$; $\mu_{17}^A = 8.012 \times 10^{-1}$; $\mu_{18}^A = -1 \times 10^{-4}$; $\mu_{19}^A = 1 \times 10^{-3}$; $\mu_{23}^A = -6.2 \times 10^{-3}$; $\mu_{24}^A = 3.1867 \times 10^{-2}$; $\mu_{25}^A = -1.556 \times 10^{-1}$; $\mu_{26}^A = 8.888 \times 10^{-1}$; $\mu_{27}^A = 0$; $\mu_{28}^A = -3.7585 \times 10^{-4}$; $\mu_{29}^A = 2.1 \times 10^{-3}$; $\mu_{34}^A = -1.01 \times 10^{-2}$; $\mu_{35}^A = 4.34 \times 10^{-2}$; $\mu_{36}^A = -1.8831 \times 10^{-1}$; $\mu_{37}^A = 9.7425 \times 10^{-1}$; $\mu_{38}^A = 0$; $\mu_{39}^A = 1 \times 10^{-4}$; $\mu_{45}^A = -8 \times 10^{-4}$; $\mu_{46}^A = 3.6 \times 10^{-3}$; $\mu_{47}^A = -1.49 \times 10^{-2}$; $\mu_{48}^A = 5.69 \times 10^{-2}$; $\mu_{49}^A = -2.217 \times 10^{-1}$; $\mu_{56}^A = 1.0624$; $\mu_{57}^A = 0$; $\mu_{58}^A = -6.2864 \times 10^{-5}$; $\mu_{59}^A = 3.0000 \times 10^{-4}$; $\mu_{67}^A = -1.4 \times 10^{-3}$; $\mu_{68}^A = 5.8806 \times 10^{-3}$; $\mu_{69}^A = -2.1 \times 10^{-2}$; $\mu_{78}^A = 7.3074 \times 10^{-2}$; $\mu_{79}^A = -2.597 \times 10^{-1}$; $\mu_{89}^A = 1.134$; $D_0^A = 0.0499$; $D_1^A = 0.3962$; $D_2^A = 0.2$; $D_3^A = 0.1009$; $D_4^A = 0.3024$; $D_5^A = 0.5$; $D_6^A = 0.45$; $D_7^A = 0.2482$; $D_8^A = 0.1499$; $D_9^A = 0.074$.

(28) Zhang, H.; Rabitz, H. unpublished, 1994.